Seasonal variation in total organic carbon in the northeast Atlantic in 2000–2001

Rumi Sohrin[1] and Richard Sempéré

Laboratoire de Microbiologie Géochimie et Ecologie Marines, CNRS/INSU, UMR 6117, Centre d'Océanologie de Marseille, Université de la Mediterranée, Marseille, France

Received 28 September 2004; revised 31 May 2005; accepted 2 June 2005; published 29 October 2005.

[1] Total organic carbon (TOC) was measured in the midlatitudes of the northeast Atlantic in 2000–2001 during the Programme Océan Multidisciplinaire Méso Echelle (POMME). In spring, mixed layer depth (MLD) was positively correlated with the north latitude, while the surface TOC and chlorophyll-*a* (Chl *a*) were negatively correlated with it. It indicates the northward propagation of TOC accumulation along the onset of spring bloom, which was triggered by shoaling of MLD from the south. Surface TOC was highest in summer, though surface Chl *a* was lowest. Surface TOC was significantly correlated with surface Chl *a* during winter and spring but not during summer or fall, indicating the minor influence of total phytoplankton biomass on surface TOC distribution in the oligotrophic season. High surface TOC in summer and fall was related with shallow MLD, which could hold fresh TOC near the surface. Downward TOC flux from the surface to below the seasonal thermocline was estimated for the processes of winter convection (F_c), turbulent diffusion (F_d) and sinking flux (F_p). The sum of these fluxes accounts for 6–75% of annual new production. To our knowledge, this is the first estimation based on the simultaneous measurement of F_c, F_d, F_p, and annual new production.

Citation: Sohrin, R., and R. Sempéré (2005), Seasonal variation in total organic carbon in the northeast Atlantic in 2000–2001, *J. Geophys. Res.*, *110*, C10S90, doi:10.1029/2004JC002731.

1. Introduction

[2] Dissolved organic carbon (DOC) in the ocean is one of the largest organic carbon reservoirs on Earth and its pool size (685–700 Gt C) is comparable to the stock of atmospheric CO_2 (750 Gt C) [*Siegenthaler and Sarmiento*, 1993; *Fasham et al.*, 2001]. DOC is directly produced as a by-product of primary production and also supplied into the water column *via* biotic and abiotic processes on particles, for example, bacterial degradation, grazing and abiotic dissolution [*Carlson*, 2001, and references therein]. Bacteria rapidly utilize a large fraction (>50%) of primary production within the upper ocean [*Cho and Azam*, 1988], but a part of DOC may accumulate in the upper ocean and then be transported horizontally elsewhere by the general circulation [*Wiebinga and de Baar*, 1998; *Dafner et al.*, 2001] or transferred to the intermediate and deep waters *via* various physical processes such as winter convection [*Copin-Montégut and Avril*, 1993; *Carlson et al.*, 1994] and turbulent diffusion [*Copin-Montégut and Avril*, 1993; *Doval et al.*, 2001]. DOC is a crucial carbon source for heterotrophic bacteria, and the mechanism and the magnitude of DOC supply is a key to understanding carbon cycle in the ocean.

[3] The temperate latitudes of the northeast Atlantic Ocean are well known as a strong sink for atmospheric CO_2 and also as the areas where thermohaline circulation influences the carbon cycle [*Sarmiento et al.*, 1995]. This area can be divided into the north and the south of 42°N according to the relatively deep (reaching about 500 m) and shallow (100–150 m) winter mixed layers, respectively [*Paillet and Arhan*, 1996]. Discontinuity in the depths of the winter mixed layer may cause difference in the spring bloom: a relatively productive one is expected in the north due to the extensive supply of nutrients by the uplift of the deeper water, whereas more oligotrophic one is expected in the south [*Mémery et al.*, 2005]. Intermediate waters (~500–2000 m) complexly comprise several water masses and their contribution varies with the site. For example, saline and warm Mediterranean Sea Outflow Water (MSW) has been traced around 1000 m and fresh Labrador Sea Water (LSW) has been traced around 1850 m along 20°W in 33°–52°N [*Tsuchiya et al.*, 1992; *van Aken*, 2000a, 2000b]. Because of a considerable overlap in the density ranges of these water masses, diapycnal and isopycnal mixing occurs in the intermediate waters [*van Aken*, 2000b]. Subduction of 11°–12°C mode waters (defined as North Atlantic Mode Water and Subpolar Mode Water by *Reverdin et al.* [2005] and *Le Cann et al.* [2005], respectively) is expected to be occurred near the front around 42°N and its southward drift is also suggestive [*Mémery et al.*, 2005, and references therein]. Furthermore, the area is characterized by a number

[1]Now at Institute of Geosciences, Shizuoka University, Shizuoka, Japan.

0148-0227/05/2004JC002731

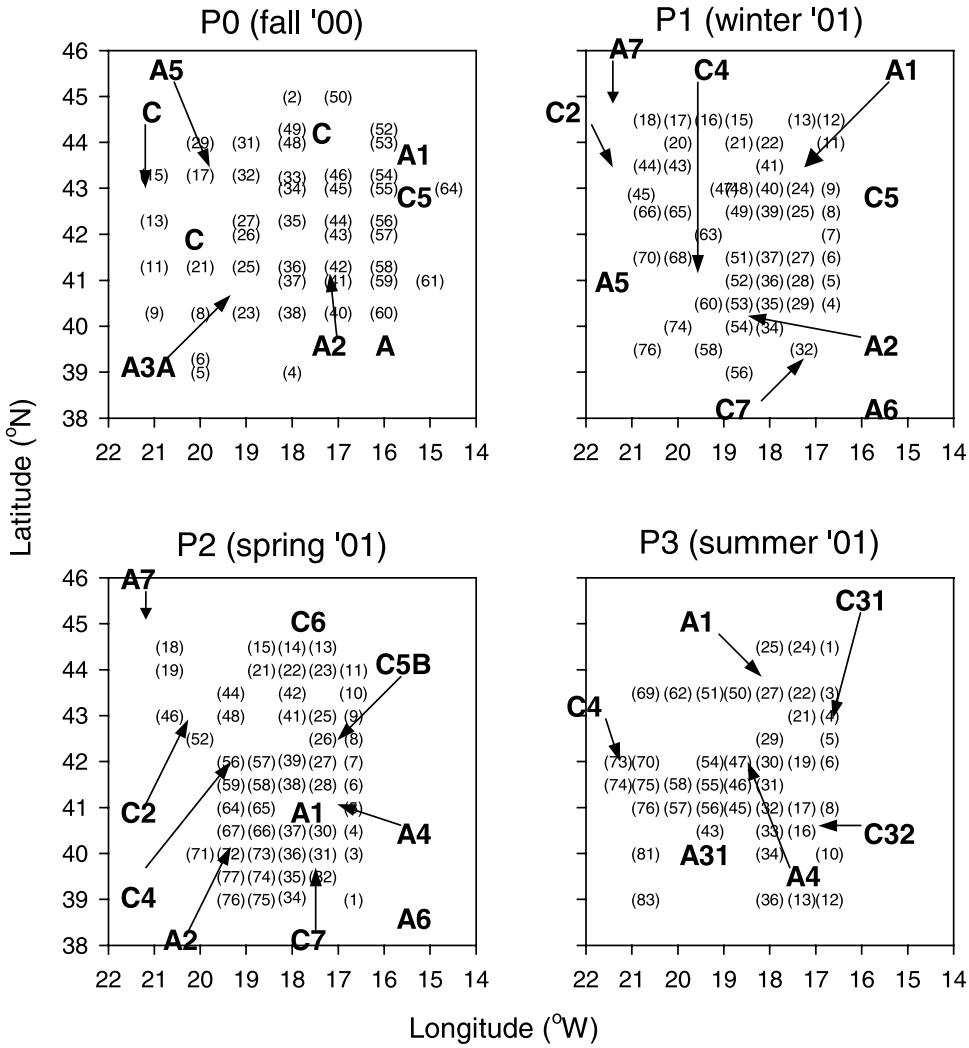

Figure 1. Stations for sampling of total organic carbon (TOC) in Programme Océan Multidisciplinaire Méso Echelle (POMME). Numbers in parentheses are the station names, which represent the order of sampling date in each cruise. Approximate location of anticyclonic (Ax) and cyclonic eddies (Cx) at 100 m is shown according to the figures of *Mémery et al.* [2005] and M. Assenbaum (LEGOS, Toulouse, http://www.omp.obs-mip.fr/omp/pomme/donnees_structures_frame.html).

of mesoscale features, i.e., anticyclonic and cyclonic eddies [*Le Cann et al.*, 2005]. These physical processes and characteristics can play an important role in vertical and horizontal transfer of DOC. Therefore to better understand carbon dynamics in the northeast Atlantic, it is important to obtain a detailed spatial distribution of DOC in a seasonal cycle. Here we report a seasonal distribution of total organic carbon (TOC) in the middle latitudes of the northeast Atlantic, especially for the surface to the intermediate waters. Seawater samples were obtained at more than 45 stations in each of four seasons in 2000–2001 during Programme Océan Multidisciplinaire Méso Echelle (POMME), covering an area of 224,000 km^2 (39°–44.5°N, 16.5°–21°W).

2. Materials and Methods

2.1. Study Area and Sampling

[4] Seawater samples were taken in the northeast Atlantic during four cruises of Programme Océan Multidisciplinaire Méso Echelle (POMME) from September 2000 to September 2001. The study area is situated between off the Iberian Peninsula and the Azores islands (39°–44.5°N, 16.5°–21°W (Figure 1)). Details of the sampling periods and the numbers of stations in each cruise are presented in Table 1. We roughly defined the seasons by the cruises; fall (P0), winter (P1), spring (P2) and summer (P3). P1, P2 and P3 included two legs (leg 1 and leg 2) whereas P0 comprised only one leg. Note that only the concentration of total organic carbon (TOC) related to the seawater samples collected during P0 and the leg 1 of P1, P2 and P3 is given in this paper. Concentrations of particulate organic carbon (POC) and TOC were measured by *Doval et al.* [2001] and *Huskin et al.* [2004] during the cruises of Azores 1 (August 1998) and Azores 2 (April 1999) in the southwest district (28°–38°N, 20°–23°W) of our study area. Using their data, the contribution of POC to TOC within the euphotic zone was evaluated as 10% and 6% during spring and summer, respectively, which suggests the small contribution of POC to our TOC samples over the observations.

Table 1. Summary of Sampling and Total Organic Carbon (TOC) Analysis in the Programme Océan Multidisciplinaire Méso Echelle (POMME) Cruises

	Sampling			TOC Analysis	
Cruise	Period (Season)	Study Area (NW End/SE End)	Number of Stations (TOC/All)[a]	Period	Number of Samples
P0	18 Sep–12 Oct 2000 (fall)	21.0°W, 45.0°N/15.0°W, 39.0°N	45/66	31 Jan–27 Jul 2001	695
P1	3–23 Feb 2001 (winter)	20.8°W, 44.5°N/16.4°W, 38.6°N	49/79	30 Jul–18 Dec 2001	485
P2	24 Mar–11 Apr 2001 (spring)	20.7°W, 44.5°N/16.7°W, 39.0°N	52/81	3 Dec 2002–25 Mar 2004	739
P3	26 Aug–13 Sep 2001 (summer)	21.3°W, 44.5°N/16.7°W, 39.0°N	45/83	1 Nov–2 Dec 2002	715
Total			191/309		2634

[a]Number of the stations where CTD was launched (all) and TOC sampling was conducted (TOC).

[5] Discrete sample waters were collected with 12 L Niskin bottles mounted on a CTD/rosette. Rubber made ribbons and o-rings of the original Niskin bottles were replaced with silicon ribbons and Viton o-rings, respectively, and the bottles were washed with 0.1 M HCl and Milli-Q water before each cruise. TOC samples were collected directly (without tubing) from the Niskin bottles into precombusted 10 mL (P0 and P3) or 5 mL (P1 and P2) glass ampoules in duplicates, first or after gas sampling to avoid organic carbon contamination. The ampoules were rinsed two times with the respective water samples before filling. Samples were immediately poisoned by the addition of 20 μl of H_3PO_4 (final pH $\sim$ 2) in a laminar flow clean air bench. The ampoules were flame sealed and stored in the dark at 4°C until the analysis. Plastic gloves were worn and care was taken to minimize contamination during sampling and the following procedure.

2.2. Total Organic Carbon (TOC) Analysis

[6] TOC concentration was measured by a high-temperature catalytic oxidation method using a modified Shimadzu TOC-5000 total carbon analyzer equipped with 1.2% platinum on silica pillows with approximate diameter of 2 mm as a catalyst [*Dafner et al.*, 2001; *Sempéré et al.*, 2003]. Four-point calibration curve was obtained daily by injecting the working solutions of potassium hydrogen phthalate which were freshly prepared every three days by diluting the stock solution with Milli-Q and then acidifying the dilutions with H_3PO_4. The stock and working solutions were kept in the dark at 4°C and the stock was available at least for one year. TOC concentration was determined by subtracting the running blank from the average peak area of the samples (n = 3 or 4) and dividing the subtraction by the slope of the calibration curve. The running blank was determined as the average of all the peak area of the Milli-Q water acidified with H_3PO_4. The acidified Milli-Q water was injected in triplicate every four samples. Low Carbon Water (LCW) and Deep Seawater Reference (DSR) distributed by D. Hansell laboratory (University of Miami) were daily measured to check the accuracy and the stability of TOC analysis.

2.3. Statistics and Computing the Variables

[7] Difference in TOC concentration among the cruises or locations was examined by one-way ANOVA with post hoc Scheffé test using Systat 10 (Systat Software Inc.) in the case of the numbers of classes > 2, whereas Student's t-test was applied in the case of the numbers of classes = 2. The level of significance of both analyses was set at 0.05.

[8] Mixed layer depth (MLD) was calculated as a depth where σ_θ exceeded the one at the surface (5 m) by 0.125 [*Levitus*, 1982]. The stability of the seasonal thermocline was estimated from the maximum of the squared Brunt-Väisälä frequency (N^2 (s^{-2})) in the upper 150 m:

$$N^2 = \frac{g}{\rho}\left(\frac{\Delta\rho}{\Delta P}\right),$$

where g is the gravity acceleration, ρ and P are the averages of density and pressure over the 5 dbar intervals, respectively, and $\Delta\rho/\Delta P$ is the corresponding density gradient. The turbulent diffusion flux of TOC across the pycnocline layer (F_d) was estimated according to *Copin-Montégut and Avril* [1993] and *Doval et al.* [2001] as follows:

$$F_d = -Kz\frac{dC}{dZ} = -\left\{\frac{\varepsilon R}{N^2_{\max}(1-R)}\right\}\frac{dC}{dZ}.$$

K_z is the turbulent diffusion coefficient (m^2 s^{-1}), dC/dZ is TOC gradient in the pycnocline (mg C m^{-4}), ε is the dissipation rate, R is the Richardson number and $N^2_{\max}$ is the maximum of N^2. Values of ε and R were set at 10^{-8} m^2 s^{-3} and 0.2, respectively [*Copin-Montégut and Avril*, 1993]. The value of dC/dZ was obtained as follows:

$$\frac{dC}{dZ} = \frac{\mathrm{TOC}_b - \mathrm{TOC}_a}{Z_b - Z_a}.$$

TOC_a and TOC_b are the TOC concentration at the top of the pycnocline (Z_a) and the bottom of the pycnoline (Z_b), respectively. Z_a was here replaced by MLD and Z_b was determined as the depth below which N^2 became smaller than a half of $N^2_{\max}$ [*Vlasenko*, 1994]. TOC_a (or TOC_b) was calculated by linear interpolation of TOC with depth using TOC at the proximate above and blow depths of Z_a (or Z_b). Although *Doval et al.* [2001] estimated TOC_a and TOC_b as the averages of TOC from the surface to Z_a and from Z_b to 200 m, respectively, we considered that this calculation would overestimate TOC_a and/or underestimate TOC_b in POMME, because of significant TOC gradient with depth in these two layers (see Figure 2 as an example). These errors result in the overestimation of absolute value of dC/dZ, and finally derive the overestimation of F_d. Chlorophyll-*a* (Chl *a*) concentration was referred to *Maixandeau et al.* [2005] and P. Raimbault (LOB, Centre d'Océanologie de Marseille, personal communication, 2001).

3. Results and Discussion

3.1. Precision and Accuracy of TOC Concentration

[9] Average TOC concentration at respective sampling depths in each cruise is shown in Table 2 as well as TOC

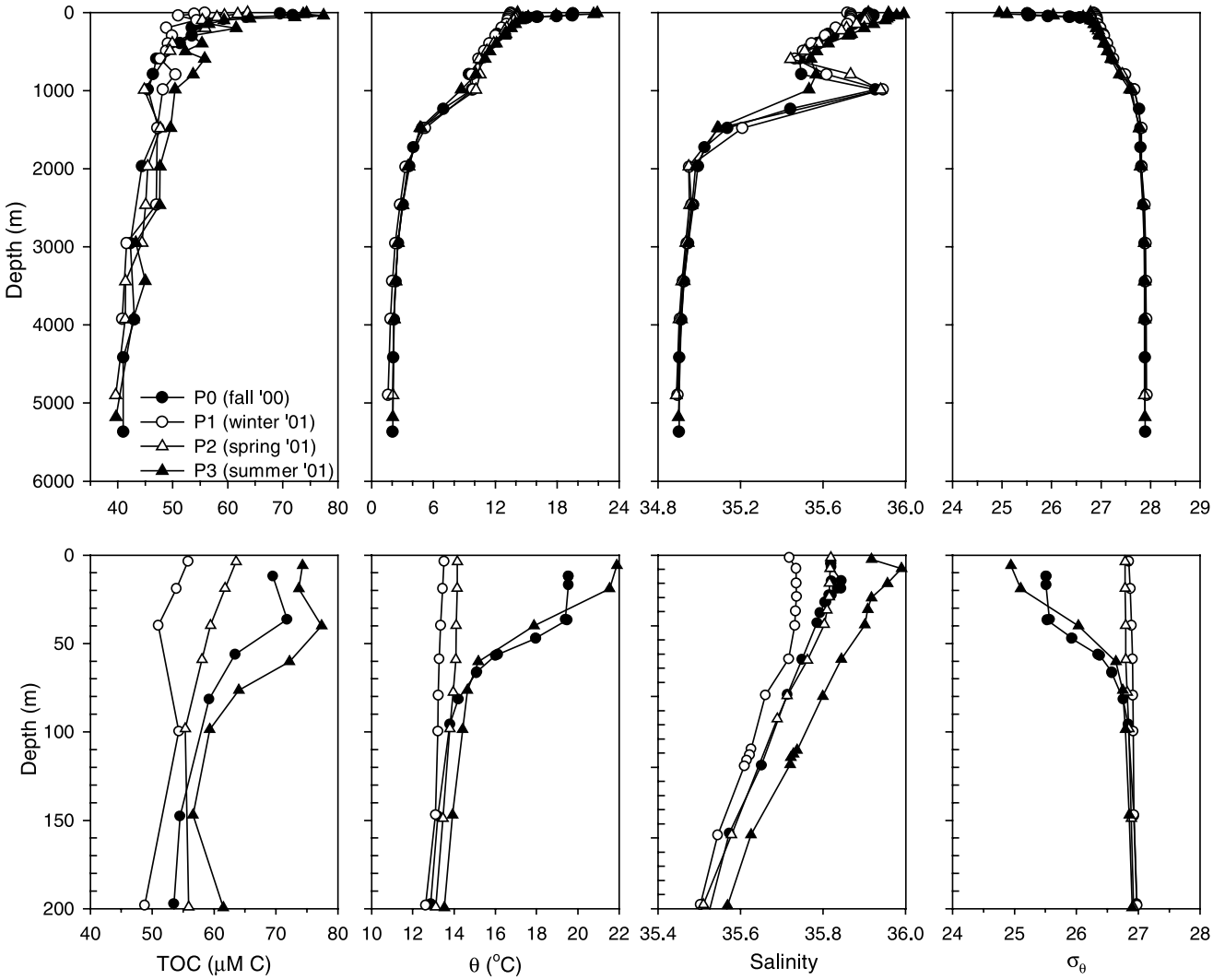

Figure 2. (top) Full-depth profiles of TOC, potential temperature (θ), salinity, and potential density anomaly (σ_θ) at 41.5°N, 18°W in each POMME cruise and (bottom) the corresponding profiles in the upper 200 m.

concentration of the references, i.e., DSR and LCW. The subtraction of LCW from DSW was 42.1–43.4 μM and is consistent with its nominal value (42.0–45.0 μM C) mentioned by D. Hansell laboratory. Precision of TOC analysis was determined as the standard deviation (sd) of triple or quadruple analysis of the same sample and the value was ±1.2 μM C on the average (n = 2326). Difference in TOC concentration between the duplicate 10 mL ampoules was 1.8 μM C on the average (n = 29), showing a good reproduction of our sampling. On the other hand, the comparison of TOC concentration between 5 mL and 10 mL ampoules in the spring cruise showed that TOC in 5 mL ampoules was significantly higher (paired Student's t-test, $P < 0.01$; n = 7) than that in 10 mL ampoules with a difference of 2.5 ± 1.5 μM C (average ± sd; range, 0.6–4.4 μM C). This result indicates the possible overestimation of TOC in winter and spring, which was likely caused by contamination and/or concentration of organic matter during flame sealing of relatively small ampoules. However, there was no significant difference ($P > 0.05$) in TOC over the cruises as to the depths below 2500 m (Table 2), suggesting that the overestimation was not systematic. Because the storage period of TOC samples varied from 4 months to 3 years among the samples (Table 1), we checked the effect of storage period on TOC concentration. This test was conducted using the surface (10–50 m) samples of the fall cruise, since the surface samples in the stratified period would contain a large amount of bioavailable organic compounds that can be easily mineralized during storage. TOC in 7-month-preserved sample was higher by 0.5 μM C on the average (n = 5) than that in 3.5-year-preserved sample, but the difference was not significant ($P > 0.5$). This result indicates that the effect of long-term storage was negligible for TOC concentration.

[10] Possibility of TOC contamination during the cruise was checked by comparing the deep (2000 m) TOC concentration between the first and the last five stations in each cruise: the difference was not significant ($P > 0.2$) except for the summer cruise. In summer, TOC was significantly ($P < 0.05$) higher by 4.1 ± 0.2 μM C in the west of

Table 2. TOC Concentration (Average ± sd (μM C)) of the Samples and the References Throughout the Analysis[a]

Cruise Period	P0, Sep–Oct 2000 (Fall 2000)	P1, Feb 2001 (Winter 2001)	P2, Mar–Apr 2001 (Spring 2001)	P3, Aug–Sep 2001 (Summer 2001)[b]	Order of TOC[c]
			Samples		
5 m	...[d]	58.0 ± 3.0 (26)	62.9 ± 5.5 (41)	74.9 ± 4.4 (24)	P3 > P2 > P1
10 m	70.0 ± 2.0 (42)	59.8 (2)	...	...	...
20 m	71.8 (2)	57.3 ± 3.0 (26)	60.9 ± 4.4 (48)	74.3 ± 5.1 (23)	P3 > P0 > P2 > P1
30 m	68.5 ± 3.0 (39)	57.4 ± 2.4 (6)	56.6 (2)	71.8 ± 4.3 (19)	P3 > P0 > (P1, P2)
40 m	66.6 ± 4.6 (4)	56.5 ± 3.3 (21)	59.9 ± 4.2 (48)	69.9 ± 6.4 (24)	(P0, P3) > (P1, P2)
50 m	62.4 ± 4.6 (36)	56.7 ± 3.1 (18)	58.7 ± 2.9 (15)	66.7 ± 6.3 (19)	P3 > (P0, P1, P2); P0 > P1
60 m	62.7 ± 3.8 (5)	56.5 ± 2.9 (15)	58.5 ± 3.9 (42)	63.0 ± 5.8 (22)	(P0, P3) > P1; P3 > P2
70 m	53.0 ± 2.1 (3)	...	...	...	...
80 m	55.6 ± 2.6 (36)	56.5 ± 3.1 (27)	57.9 ± 3.4 (44)	57.9 ± 3.5 (23)	P2 > P0
100 m	53.7 ± 2.1 (36)	56.4 ± 3.3 (33)	57.2 ± 4.3 (46)	56.4 ± 2.7 (23)	(P1, P2, P3) > P0
150 m	53.0 ± 2.0 (38)	57.8 (2)	55.1 ± 3.2 (45)	53.9 ± 2.6 (23)	P2 > P0
200 m	51.8 ± 1.7 (40)	54.4 ± 3.0 (34)	53.7 ± 2.6 (49)	53.7 ± 3.4 (24)	(P1, P2, P3) > P0
300 m	50.7 ± 1.7 (41)	51.4 ± 2.6 (36)	52.2 ± 2.7 (48)	52.0 ± 2.9 (23)	ns[e]
400 m	49.6 ± 1.9 (41)	50.4 ± 2.2 (33)	51.3 ± 2.8 (49)	50.8 ± 3.0 (24)	P2 > P0
500 m	49.0 ± 2.0 (34)	50.3 ± 3.2 (40)	49.7 ± 3.1 (46)	50.1 ± 2.0 (7)	ns
600 m	48.1 ± 1.9 (43)	49.5 ± 4.4 (35)	48.5 ± 2.7 (45)	49.3 ± 3.6 (23)	ns
800 m	45.6 ± 1.8 (42)	47.1 ± 3.3 (44)	46.5 ± 2.6 (48)	47.9 ± 3.6 (24)	P3 > P0
1000 m	44.9 ± 1.7 (42)	46.3 ± 2.2 (42)	46.0 ± 3.6 (50)	46.2 ± 3.8 (23)	ns
1250 m	44.9 ± 0.6 (3)	...	...	...	...
1500 m	45.1 ± 1.6 (42)	46.0 ± 2.6 (39)	45.2 ± 2.3 (45)	47.2 ± 3.4 (24)	P3 > (P0, P2)
1750 m	44.5 (2)	...	...	...	...
2000 m	44.7 ± 0.7 (42)	46.5 ± 2.6 (15)	44.5 ± 1.9 (34)	45.9 ± 2.5 (18)	P1 > (P0, P2)
2500 m	...	44.9 ± 3.7 (3)	44.6 ± 2.1 (7)	45.6 ± 1.8 (3)	ns
3000 m	42.8 ± 1.5 (21)	43.6 ± 2.9 (5)	42.2 ± 1.4 (7)	42.8 ± 2.6 (5)	ns
3500 m	42.6 ± 3.0 (3)	42.4 ± 2.8 (3)	41.2 ± 0.8 (7)	43.6 ± 2.3 (4)	ns
4000 m	42.3 ± 1.8 (19)	41.1 ± 2.0 (5)	41.3 ± 1.2 (7)	42.5 ± 0.3 (3)	ns
4001–4500 m	40.7 ± 1.2 (17)	41.3 (2)	40.4 (2)	...	ns
4501–5000 m	40.4 ± 1.5 (13)	...	40.4 ± 1.6 (5)	...	ns
5001–5368 m	40.9 ± 1.2 (9)	...	...	...	...
			References[f]		
DSW	43.1 ± 0.9 (45)	43.5 ± 1.1 (46)	43.1 ± 1.4 (52)	42.1 ± 0.6 (45)	
LCW	1.1 ± 1.0 (43)	1.0 ± 1.6 (46)	−0.3 ± 1.2 (52)	−1.0 ± 1.3 (45)	

[a]Numbers of the stations (samples) and the analyses (references) are in parentheses.
[b]Data in the east of 18°W.
[c]Difference was examined by one-way ANOVA with a post hoc Scheffé test ($\alpha = 0.05$).
[d]Not determined or examined.
[e]Not significant difference.
[f]Deep Seawater Reference (DSW) and Low Carbon Water (LCW) supplied by D. Hansell laboratory (University of Miami).

18°W (>18°W) than in the east (≤18°W) at the respective depths below 30 m. This result suggests the contamination of organic carbon or spatial difference in TOC during the summer cruise, because the stations have been arranged in the order of the west longitude (Figure 1). In other cruises, TOC in the west of 18°W was not significantly higher than that in the east of 18°W. We cannot contradict the contamination of organic carbon in the west of 18°W during the summer cruise, and thus summer TOC data are shown only for those in the east of 18°W.

3.2. Hydrological Characteristics of the Water Column

[11] Depth profiles of TOC, potential temperature (θ), salinity and potential density anomaly (σ_θ) at 41.5°N, 18°W during each cruise are shown in Figure 2. Both salinity and temperature maximum were observed at 1000 m, attesting a mark of Mediterranean Sea Outflow Water (MSW) [*Tsuchiya et al.*, 1992; *van Aken*, 2000a, 2000b]. Salinity minimum around 2000 m is considered as a core of Labrador Sea Water (LSW) [*van Aken*, 2000a]. Seasonal thermocline was found between 40 m and 80 m in fall and between 20 m and 60 m in summer. TOC was slightly high at 40 m and then decreased rapidly toward 100 m in summer and fall, indicating an accumulation of TOC above the seasonal thermocline during the stratified period.

3.3. TOC Distribution in the Surface Water

[12] North-south trends of MLD and the depth-integrated Chl *a* (10–30 m) as well as that of TOC (10–30 m) are shown in Figure 3, and those averages are summarized in Table 3 as well as the average of integrated Chl *a* in 10–300 m. Integrated Chl *a* in 10–300 m represents the total Chl *a* stock in the water column, because the euphotic layer depth was shallower than 120 m in the whole area over the cruises [*Fernández I. et al.*, 2005]. On the other hand, integrations between 10 m and 30 m characterizes the stocks above the seasonal thermocline in summer, because summer MLD was 26 ± 8 m (Table 3). Along the latitudes of 39°–39.5°N in the spring cruise, MLD was significantly shallower ($P < 0.001$) at stations 75–81 (20–40 m; 10–12 April) than that at the former stations along the same latitudes (84–144 m), indicating that stratification was likely to start in the beginning of April. The TL6 CLIPPER model demonstrated rapid MLD shoaling between the beginning and the middle of April in the whole POMME area [*Lévy et al.*, 2005]. The model predicted that MLD reached 80 m between 20

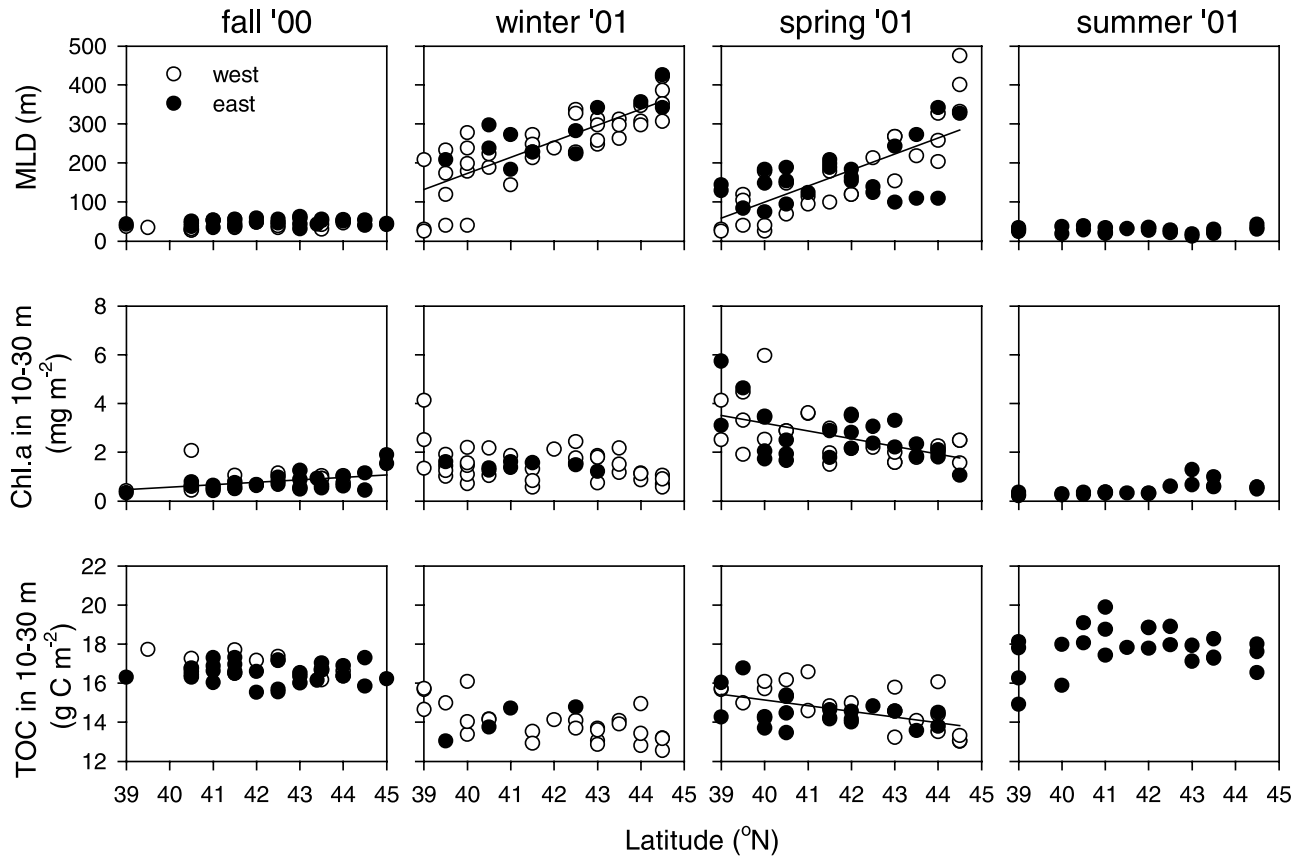

Figure 3. (top) North-south trends of the mixed layer depth (MLD), (middle) chlorophyll-*a* (Chl *a*) stock in 10–30 m, and (bottom) TOC stock in 10–30 m from fall 2000 to summer 2001. Filled circles present data east of 18°W (east), and open circles present data west of 18°W (west). Line indicates a linear regression between the variables and the north latitude at a significant level $\alpha = 0.05$. Note that the variables are shown only in east during summer.

November 2000 (45°N) and 5 January 2001 (39°N) (estimated date from *Lévy et al.* [2005, Figure 2]). Thus we estimated the duration of winter mixing as 3 months for 39°N, 5 months for 45°N and assumed the linear propagation of the start of winter mixing with the north latitude between 39°N and 45°N. In winter and spring, MLD was significantly higher in the north of 41°N (≥41°N) than in the south (<41°N) (Table 3). On the basis of the Sea-viewing Wide Field-of-view Sensor (SeaWiFS) ocean color images and the predicted MLD by the model, *Lévy et al.* [2005] defined the north of 41.2°N as the subpolar region and 36.2°–41.2°N as the midlatitude region: the subpolar region had distinct blooms in spring and fall, whereas the midlatitude region had a relatively small bloom starting in fall. The subpolar spring bloom is considered to be triggered by shoaling of MLD to the depth shallower than 180 m which was the twice the euphotic layer depth in that region [*Lévy et al.*, 2005]. In the south of 41°N during spring, MLD was shallower than 188 m and the total Chl *a* stock was significantly higher (7.7 ± 2.1 mg m^{-2}; $P < 0.05$) than that in the north of 41°N (6.4 ± 1.7 mg m^{-2}) where MLD reached 475 m (Figure 3, Table 3). This result suggests the onset of the spring bloom in the south of 41°N by restratification. The surface (10–30 m) stocks of both TOC and Chl *a* were significantly correlated to the north latitude (adjusted squared correlation coefficient (r^2) = 0.28 and 0.29, respectively, $P < 0.001$) during spring and they marked the significantly ($P < 0.05$) higher values in the south of 41°N than those in the north of 41°N (Figure 3, Table 3). Surface Chl *a* stock was positively ($r = 0.41$, $P < 0.01$) correlated to the north latitude during fall, but there

Table 3. Mixed Layer Depth (MLD), Integrated Chlorophyll-*a* (Chl *a*), and Integrated TOC in the Whole Area and the North and the South of 41°N (Average ± sd)[a]

Cruise (Period)	Region	MLD, m	Chl *a*, mg m^{-2}		TOC (10–30 m), g C m^{-2}
			10–300 m	10–30 m	
P0 (fall 2000)	whole	45 ± 9	4.0 ± 1.2	1.9 ± 1.4	16.9 ± 1.0
	north	46 ± 9	3.9 ± 1.2	1.8 ± 1.1	16.9 ± 1.0
	south	40 ± 7	4.6 ± 1.0	2.3 ± 1.9	16.6 ± 1.1
P1 (winter 2001)	whole	274 ± 64	4.0 ± 1.0	1.6 ± 0.8	13.7 ± 0.6
	north	**290 ± 64**	**4.3 ± 1.0**	**1.4 ± 0.5**	13.6 ± 0.7
	south	**224 ± 35**	**3.4 ± 0.7**	**2.0 ± 1.0**	13.9 ± 0.5
P2 (spring 2001)	whole	169 ± 97	6.9 ± 2.0	2.7 ± 1.0	14.4 ± 1.0
	north	**207 ± 96**	**6.4 ± 1.7**	**2.3 ± 0.7**	**15.1 ± 0.9**
	south	**104 ± 56**	**7.7 ± 2.1**	**3.2 ± 1.3**	**17.6 ± 1.0**
P3 (summer 2001)[b]	whole	26 ± 8	2.6 ± 0.7	0.5 ± 0.3	17.6 ± 1.2
	north	26 ± 9	2.8 ± 0.6	**0.5 ± 0.3**	18.0 ± 0.9
	south	26 ± 5	2.1 ± 0.8	**0.3 ± 0.0**	16.6 ± 1.4

[a]Boldface represents the significant difference between the north and the south.
[b]Data in the east of 18°W.

were no significant correlations between the north latitude and the surface stocks of Chl *a* or TOC in other seasons.

[13] Simple linear regression exhibited a positive correlation between the surface stocks of TOC and Chl *a* in winter and spring (r^2 = 0.46 and 0.27, respectively, $P < 0.001$), while there was no significant correlation in summer or fall (r^2 = 0.0, $P > 0.5$). On the other hand, negative correlation ($r = -0.38$ to -0.53, $P < 0.05$) was found between surface TOC stock and MLD during fall, winter and spring. The negative correlation between the surface TOC stock and MLD could be related to the restriction of freshly supplied TOC within the mixed layer, i.e., deeper MLD disperses the fresh TOC within a thicker layer, which decreases the surface TOC concentration [*Tanoue*, 1993; *Hansell and Carlson*, 2001]. Also, deep MLD facilitates a mixing of the surface water with a large volume of deep water with low TOC content [*Hansell and Carlson*, 2001]. The positive correlation between the surface stocks of TOC and Chl *a* in winter and spring means that more TOC was accumulated within the surface water in the progress of the spring bloom. In this case, the progress of spring bloom was occurred along the shoaling of MLD (Figure 3), which also worked to keep the surface TOC level high. On the other hand, no significant correlation in summer or fall between surface TOC and Chl *a* indicates the minor influence of total phytoplankton biomass on surface TOC distribution in the oligotrophic season.

[14] Surface TOC stock was largest in summer, although surface Chl *a* stock was lowest (Table 3, Figure 3). The high surface TOC in summer would result from the shallow MLD, but it might be partly related to high abundance of picophytoplanton. *Teira et al.* [2001] reported the large supply of dissolved organic carbon (DOC) via primary production in the oligotrophic North Atlantic subtropical gyre, where picophytoplankton dominated. In POMME, picoplankton was dominant (53%) in phytoplankton biomass during summer, whereas their contribution was relatively small (44% and 22%) during winter and spring [*Claustre et al.*, 2005]. It should be noted that *Fernández I. et al.* [2005] reported the higher regenerated production (assimilation of ammonium, >4 mmol m^{-2} d^{-1}) in the area of 40.5°–43°N, 16.7°–17.3°W compared to the other area during summer. Surface TOC stock was also relatively large in 40.5°–42.5°N of the east of 18°W during summer (Figure 3), although the maximums of surface Chl *a* stock (Figure 3) and new production [*Fernández I. et al.*, 2005] were shown at 43°N and MLD was distributed rather uniformly in the east of 18°W (Figure 3). In the upper 30 m, *f* ratio (ratio of new production to the sum of new production and regenerated production) was lower during summer (<0.1) than during winter and spring (0.4–0.5, respectively), indicating larger contribution of regenerated production to primary production during summer than during winter and spring [*Fernández I. et al.*, 2005]. Therefore spatial distribution of surface TOC stock could be related to regenerated production in summer due to the relatively low background of new production compared to other seasons.

3.4. TOC Distribution in the Subsurface and Intermediate Waters

[15] In contradiction to the surface water, TOC was significantly higher in winter or spring than in fall between 80 and 400 m (Table 2, Figure 2). The depth where the trend changed from the surface is just below the bottom of the pycnocline (80 m (Figure 2)), suggesting an entrainment of surface TOC below the seasonal themocline by winter convection. Largest TOC variation in 80–400 m was found at 150 m (Table 2). TOC at 150 m decreased from 57.8 μM C in winter to 53.9 μM C in summer, the latter of which is close to the TOC level in fall (53.0 μM C) (Table 2). This decrease means not only the stop of TOC entrainment due to shoaling of MLD but also consumption and/or export of TOC during winter and summer. Assuming a linear TOC decrease with time, 3.9 μmol C L^{-1} of TOC decrease between winter and summer (~6 months (Table 1)) gives 22 nmol C L^{-1} d^{-1} of TOC decrease rate. It is on the same order of magnitude as bacterial respiration rate during the incubation of the samples taken from 200 m in winter and summer in POMME (38 ± 20 nmol C L^{-1} d^{-1} (F. Van Wambeke, manuscript in preparation, 2005)). This result supports the hypothesis that newly entrained TOC via winter convection is an important energy source for bacteria in the subsurface water [*Carlson et al.*, 1994].

[16] Table 4 summarized TOC stock in the surface (10–80 m), subsurface (between the below of the themocline in the stratified period and the averaged winter MLD; 80–300 m) and intermediate (300–600 m) layers, as well as the layers related with MSW (600–1000 m) and LSW (1000–2000 m). Average TOC stock in the surface layer was 53.5 g C m^{-2} and 47.3 g C m^{-2} in fall and winter, respectively, showing 6.2 g C m^{-2} of net decrease between these seasons (Table 4). On the other hand, average TOC stocks in the subsurface layer increased by 5.2 g C m^{-2}. These results suggest that extra 5.2 g C m^{-2} had been accrued in the subsurface layer by winter convection and that 1.0 g C m^{-2} of TOC had been lost from the surface and the subsurface layers between fall and winter, likely by mineralization or horizontal transport. It should be noted that dissolution rate of sinking particles in the subsurface layer during winter was estimated as 0.77 mg C m^{-2} d^{-1} by multiplying the maximum difference in winter sinking flux of total carbon between 200 m and 400 m (1.3 mg C m^{-2} d^{-1} [*Goutx et al.*, 2005]) by the ratio of organic carbon to total carbon of sinking particles at 400 m (59% in winter (N. Leblond, Laboratoire d' Océanographie de Villefranche, personal communication, 2003)). This estimate is equal to total dissolution of 92 mg C m^{-2} between fall and winter(= 0.77 mg C m^{-2} d^{-1} × 120 days (approximate interval between fall and winter cruises (Table 1))), and it accounts for 3% of the net TOC increase between 200 and 400 m in the same period, suggesting the minor contribution of the dissolution of sinking particles to the enrichment of TOC in the subsurface water.

[17] The parameters for estimation of turbulent diffusion flux of TOC (F_d) is shown in Table 5. Daily F_d was 25 ± 13 mg C m^{-2} d^{-1} and 34 ± 24 mg C m^{-2} d^{-1} in fall and summer, respectively. Although the stability of the water column (N^2_{max}) was significantly larger ($P < 0.001$) in fall ((3.0 ± 0.8) × 10^{-5} s^{-2}) than in summer ((2.4 ± 0.5) × 10^{-5} s^{-2}), daily F_d had no significant difference between these seasons due to the large difference in dC/dZ among the stations (Table 5). *Doval et al.* [2001] estimated daily F_d in the transitional northeast Atlantic as 2.3 mg C m^{-2} d^{-1} (August) to 53 mg C m^{-2} d^{-1} (April) which

Table 4. TOC Stock (Average ± sd (g C m^{-2})) in the Water Column During the POMME Cruise[a]

Layer (Depth Range, m)	P0 (Fall 2000)	P1 (Winter 2001)	P2 (Spring 2001)	P3 (Summer 2001)[b]	Order of TOC Stock[c]
Surface (10–80)	53.5 ± 2.2 (42)	47.3 ± 3.5 (28)	50.0 ± 2.7 (42)	55.9 ± 3.0 (16)	(P0, P3) > P2 > P1
Subsurface (80–300)	138 ± 3 (45)	143 ± 6 (42)	144 ± 6 (52)	141 ± 6 (16)	(P1, P2) > P0
Intermediate (300–600)	177 ± 4 (42)	180 ± 7 (28)	183 ± 10 (42)	179 ± 10 (16)	ns[d]
MSW[e] (600–1000)	221 ± 6 (42)	229 ± 13 (28)	227 ± 14 (42)	226 ± 16 (16)	ns
LSW[f] (1000–2000)	540 ± 13 (44)	556 ± 24 (17)	543 ± 25 (34)	549 ± 31 (12)	ns
Whole (10–2000)	1129 ± 18 (42)	1127 ± 35 (6)	1151 ± 55 (26)	1152 ± 64 (11)	ns

[a]Numbers of stations are in parentheses.
[b]Data in the east of 18°W.
[c]Difference was examined by one-way ANOVA with a post hoc Scheffé test ($\alpha = 0.05$).
[d]Not significant difference.
[e]Mediterranean Sea Outflow Water.
[f]Labrador Sea Water.

is on the same order of magnitude as our estimate (Table 5). It should be noted that F_d of *Doval et al.* [2001] would tend to be overestimated, because the possible overestimation of the absolute value of dC/dZ as described in section 2.3.

[18] Table 6 shows the previous estimates of entrainment of TOC or DOC below the surface layer by winter convection (F_c), sinking particles (F_p) and F_d. Because the winter convection in 2001 seems to have been initiated in November at 45°N and in January at 39°N and finished in the beginning of April (see section 3.3), the annual F_d in POMME (6.8 ± 4.3 g C m^{-2} yr^{-1}) was evaluated by multiplying the average of daily F_d in summer and fall (28 mg C m^{-2} d^{-1} (Table 5)) by the stratified period (7–9 months depending on the north latitude). F_c was estimated as the difference in TOC stock in the subsurface layer between fall and winter at 22 stations whose position was identical between these periods. F_c was 5.4 ± 5.7 g C m^{-2} yr^{-1}, being consistent with the rough estimate (5.2 g C m^{-2} yr^{-1}) obtained by difference in the averaged TOC stocks over the area between these seasons as described above (see Table 4). F_c in the previous studies ranged from 4.8 g C m^{-2} yr^{-1} (minimum estimate in the Sargasso Sea [*Hansell and Carlson*, 2001]) to 26 g C m^{-2} yr^{-1} (Labrador Sea [*Tian et al.*, 2004]) and our result (5.4 g C m^{-2}) is in their lower range. It should be noted that our F_c estimate might be overestimated due to the possible TOC contamination (by 2.5 ± 1.5 μM C) derived from the use of small ampoules in winter as indicated above. In POMME, F_c was almost equal to F_d and F_p (6.0 g C m^{-2} yr^{-1} [*Guieu et al.*, 2005]). In the previous studies, F_c was reported as similar (Sargasso Sea [*Carlson et al.*, 1994]; East China Sea [*Ogawa et al.*, 2003]) or larger than F_p (Labrador Sea [*Tian et al.*, 2004]), showing the important role of winter convection in entrainment of organic carbon below the pycnocline. The contribution of F_c, F_d and F_p to annual new production (58.3 g C m^{-2} yr^{-1} [*Fernández I. et al.*, 2005]) in POMME was 0–32% (average 9.3%), −3–32% (average 12%) and 9–12% (average 10%), respectively (Table 6). The sum of these fluxes accounts for 6–75% (37 ± 14%) of annual new production. To our knowledge, this is the first result based on the simultaneous estimation of F_c, F_d, F_p, and annual new production. Given 18 g C m^{-2} yr^{-1} of a Mediterranean Sea new production [*Copin-Montégut and Avril*, 1993], which is the average of new production reported in the previous literatures, the sum of F_c, F_d and F_p accounts for 141% of new production (Table 6). The sum of F_c and F_p was 10–42% (average 19%) in POMME, while the corresponding value ranged between 40 and 69% in the other areas [*Carlson et al.*, 1994; *Tian et al.*, 2004] (Table 6), suggesting the relatively low contribution of F_c and F_p to new production in POMME. It would be partly related with inaccuracy of the various assumptions. Estimation of F_c was based on the assumption of the steady state of the water in 80–300 m from fall to winter. If the low-DOC water was advected in this layer during winter, our F_c would be underestimated. Also, our F_p is likely underestimated for the sinking flux just below the bottom of pycnocline (80 m), because sinking flux of organic carbon was available at 400 m and a substantial fraction of sinking particles should have been lost by mineralization while the particles were exported from 80 m to 400 m.

[19] Other possible processes of TOC enrichment in the subsurface water are lateral transport such as Ekman transport [*Doval et al.*, 2001] and horizontal advection related with subduction, as well as eddy-derived event (eddy pumping). Subpolar Mode Water (SPMW) is formed in the North Atlantic by winter convection and it is characterized by the minimum potential vorticity in 100–500 m, 11°–12°C and σ_θ = 27.1 along 20°W in 40°–45°N [*McCartney and Talley*, 1982; *Tsuchiya et al.*, 1992]. *Reverdin et al.* [2005] found the minimum N^2 on σ_θ = 27.10 at 41°N in both winter and spring, where the temperature was 11.70°–11.75°C, suggesting the existence of SPMW around 41°N. Figure 4 shows the vertical TOC

Table 5. Parameters in the Estimation of the Turbulent Diffusion Flux of TOC (F_d) in the Stratified Period[a]

Cruise (Period)	Z_a, m	Z_b, m	TOC at Z_a, μM C	TOC at Z_b, μM C	N^2_{max}, 10^{-5} s^{-2}	K_z, m^2 d^{-1}	dC/dZ, mg C m^{-4}	F_d, mg C m^{-2} d^{-1}
P0 (fall 2000)	45 ± 9	60 ± 8	62.8 ± 10.7	58.8 ± 9.9	3.0 ± 0.8	7.7 ± 2.2	−3.3 ± 1.8	25 ± 13
P3 (summer 2001)[b]	28 ± 8	58 ± 9	73.2 ± 4.7	64.1 ± 5.3	2.4 ± 0.5	9.7 ± 2.4	−3.6 ± 2.5	34 ± 24
Average of all	39 ± 12	59 ± 9	66.6 ± 10.2	60.7 ± 8.8	2.8 ± 0.8	8.4 ± 2.5	−3.4 ± 2.1	28 ± 18

[a]Abbreviations are as follows: Z_a, Z_b, depth of the top and the bottom of the pycnocline layer, respectively; N_{max}^2, maximum of squared Brunt-Väisälä frequency in the upper 150 m; K_z, turbulent diffusion coefficient; dC/dZ, TOC gradient in the pycnocline.
[b]Values in the east of 18°W.

Table 6. Estimations of Downward Export Flux of Organic Carbon via Winter Convection (F_c), Turbulent Diffusion (F_d), and Sinking Particles (F_p) From the Surface Layer and Their Contribution to New Production

Regions	F_c		F_d, g C m^{-2} yr^{-1}	F_p, g C m^{-2} yr^{-1}	New Production, %			Method of F_c Estimation	Reference
	g C m^{-2} yr^{-1}	Layer, m			F_c	F_d	F_p		
Sargasso Sea	4.8–14.4	100–250	...	...	...	...	...	Increase in TOC stock in 100–250 m during winter from the base TOC; the latter was estimated from the regression between time versus minimum TOC in summer and fall.	*Hansell and Carlson* [2001]
Sargasso Sea	11.9–14.5	100–250	...	8.5–15.8	23–42	...	17–27	Increase in TOC stock in 100–250 m during spring from the annual average.	*Carlson et al.* [1994]
Mediterranean Sea	14.8	<100	3.6	4–7	82	20	22–39	Decrease in DOC stock in the upper 100 m from fall to winter.	*Copin-Montégut and Avril* [1993]
Labrador Sea	26	<200	...	12.6	37	...	18	Simulation of production and consumption of DOC and suspended POC in the euphotic zone and the strength of winter convection.	*Tian et al.* [2004]
East China Sea	13	100–200	...	7–15	12	...	20	Increase in TOC stock in 100–200 m from autumn to spring.	*Ogawa et al.* [2003]
Northeast Atlantic (Azores front)	...	<200	0.69–15.9	...	...	1–26.5	63	...	*Doval et al.* [2001]
Transitional northeast Atlantic (average)	0–18 (5.4 ± 5.7)	80–300	−1.8–18.7 (6.8 ± 4.3)	5.3–6.7 (6.0)	0–32 (9.3)	−3–32 (12)	9–12 (10)	Increase in TOC stock in 80–300 m between fall and the following winter.	this study

distribution over the season in POMME as well as the depth of 11°–12°C water. The 11°–12°C water was observed in 300–500 m over the cruises (Figure 4). TOC was quite constant in 300–500 m thought the study period and over the whole area (Table 2), and thus estimation of horizontal TOC transport is still challenging from distribution of TOC. On the other hand, the isoline of TOC = 50 μM C was observed in 11°–12°C water, and it deepened in winter (Figure 4). The result suggests the subduction of the water with TOC = 50 μM C in winter and implies the possibility to trace SPMW by TOC = 50 μM C. *Reverdin et al.* [2005] and *Le Cann et al.* [2005] discussed the relation of SPMW subduction with mesoscale eddies. Regarding eddy pumping, high DOC concentration between 100 and 150 m was found near the anticyclonic eddy in the coastal transition zone of the Canary islands [*Arístegui et al.*, 2003], suggesting entrainment of high-DOC-containing water by anticyclonic eddy. On the other hand, *Doval et al.* [2001] reported similar TOC concentration in the cyclonic eddies to that in the surrounding water in the transitional northeast Atlantic. We obtained a large number of TOC data (Table 1), but they rarely matched with the core of the mesoscale eddies (Figure 1). Therefore the magnitude of eddy-pumping TOC flux could not be estimated directly from TOC distribution in POMME.

4. Conclusion

[20] TOC stock in the surface water (10–30 m) was negatively correlated with the north latitude during spring, whereas there was no significant north-south trend in other seasons (Figure 3). Combined with negative correlation between surface Chl *a* stock and the north latitude as well as positive correlation between MLD and the north latitude in spring (Figure 3), this result suggests that TOC accumulation was propagated from the south to the north along the onset of spring bloom which was triggered by shoaling of MLD from the south. In summer, surface TOC stock marked the largest value over the seasons, though surface Chl *a* stock was lowest. It would mostly relate to the shallow MLD which restricts the freshly supplied TOC near the surface. Surface TOC stock was positively correlated with the surface Chl *a* stock in winter and spring. This means that more TOC was accumulated within the surface water in the progress of spring bloom. Shallower MLD in the zone of high Chl *a* (Figure 3) also worked to keep surface TOC high. On the other hand, the correlation was not significant in summer or fall, indicating the minor influence of total phytoplankton biomass on the surface TOC distribution in the oligotorophic season. In summer, surface TOC exhibited the maximum at 40.5°–42.5°N (Figure 3) where regenerated production was highest [*Fernández I. et al.*, 2005]. This indicates the potential impact of regenerated production on surface TOC distribution in the oligotrophic season.

[21] Entrainment of TOC below the seasonal themocline was estimated for the processes of winter convection (F_c) and turbulent diffusion (F_d), and compared them to sinking flux (F_p) (Table 6). We found the similarity among F_c (5.4 ± 5.7 g C m^{-2} yr^{-1}), F_d (6.8 ± 4.3 g C m^{-2} yr^{-1}) and F_p (6.0 g C m^{-2} yr^{-1} [*Guieu et al.*, 2005]). The sum of those fluxes accounts for 6–75% (37 ± 14%) of annual new

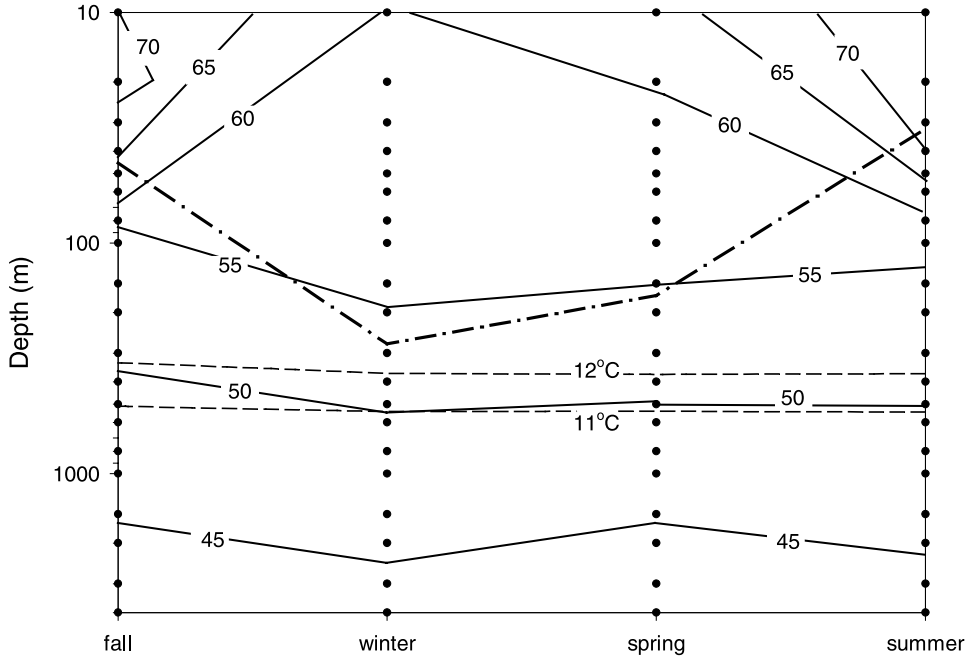

Figure 4. Contour plot of TOC on *z-t* surface over the cruises. Dash-dotted line shows MLD, and the two dashed lines represent the depth of 11°–12°C. Contour interval is 5 μM C. Note that TOC data are shown in the east of 18°W during summer.

production, suggesting the significant contribution of other processes like lateral transport (Ekman transport and subduction-derived advection) and eddy pumping to entrain TOC into the subsurface layer.

[22] **Acknowledgments.** We thank the officers and crew of the R/V *L'Atalante* and R/V *Thalassa* for their valuable assistance and support. We also thank J. Raunet and D. Tailliez for CTD operations and C. Guigue and C. Magen for sample collections. We are also grateful to the leaders of the POMME program (L. Mémery and G. Reverdin) and the three chief scientists (Y. Desaubies, M. Bianchi, and L. Prieur) of the cruises of P0 and legs 1 in P1–P3. We acknowledge comments on the manuscript by L. Mémery, G. Reverdin, M. Roy-Barman, C. Panagiotopoulos, and two anonymous reviewers and P. Raimbault and F. Van Wambeke for providing data of Chl *a* and bacterial respiration. This research was funded by the POMME program in the framework of the PROOF project from CNRS/INSU, France. R. Sohrin was supported by Ministère de la l'Education et de la Recherche and CNRS.

References

Arístegui, J., E. D. Barton, M. F. Montero, M. García-Muñoz, and J. Escánez (2003), Organic carbon distribution and water column respiration in the NW Africa-Canaries coastal transition zone, *Aquat. Microbial Ecol.*, *33*, 289–301.

Carlson, C. A. (2001), Production and removal processes, in *Biogeochemistry of Marine Dissolved Organic Matter*, edited by D. A. Hansell and C. A. Carlson, pp. 91–151, Elsevier, New York.

Carlson, C. A., H. W. Ducklow, and A. F. Michaels (1994), Annual flux of dissolved organic carbon from the eutrophic zone in the northwestern Sargasso Sea, *Nature*, *371*, 405–408.

Cho, B. C., and F. Azam (1988), Major role of bacteria in biogeochemical fluxes in the ocean's interior, *Nature*, *332*, 441–443.

Claustre, H., M. Babin, D. Merien, J. Ras, L. Prieur, S. Dallot, O. Prasil, H. Dousova, and T. Moutin (2005), Toward a taxon-specific parameterization of bio-optical models of primary production: A case study in the North Atlantic, *J. Geophys. Res.*, *110*, C07S12, doi:10.1029/2004JC002634.

Copin-Montégut, G., and B. Avril (1993), Vertical distribution and temporal variation of dissolved organic carbon in the north-western Mediterranean Sea, *Deep Sea Res., Part I*, *40*, 1963–1972.

Dafner, E. V., R. Sempéré, and H. L. Bryden (2001), Total organic carbon distribution and budget through the Strait of Gibraltar in April 1998, *Mar. Chem.*, *73*, 233–252.

Doval, M. D., X. A. Álvarez-Salgado, and F. F. Pérez (2001), Organic matter distributions in the eastern North Atlantic–Azores Front region, *J. Mar. Syst.*, *30*, 33–49.

Fasham, M. J. R., et al. (2001), A new vision of ocean biogeochemistry after a decade of the Joint Global Ocean Flux Study (JGOFS), *Ambio*, *10*, 4–31.

Fernández I., C., P. Raimbault, N. Garcia, P. Rimmelin, and G. Caniaux (2005), An estimation of annual new production and carbon fluxes in the northeast Atlantic Ocean during 2001, *J. Geophys. Res.*, *110*, C07S13, doi:10.1029/2004JC002616.

Goutx, M., C. Guigue, N. Leblond, A. Desnves, D. Aritio, and C. Guieu (2005), Particle flux in the northeast Atlantic Ocean during the POMME experiment (2001): Results from mass, carbon, nitrogen, and lipid biomarkers from the drifting sediment traps, *J. Geophys. Res.*, *110*, C07S20, doi:10.1029/2004JC002749.

Guieu, C., M. Roy-Barman, N. Leblond, C. Jeandel, M. Souhaut, B. Le Cann, A. Dufour, and C. Bournot (2005), Vertical particle flux in the northeast Atlantic Ocean (POMME experiment), *J. Geophys. Res.*, *110*, C07S18, doi:10.1029/2004JC002672.

Hansell, D. A., and C. A. Carlson (2001), Biogeochemistry of total organic carbon and nitrogen in the Sargasso Sea: Control by convective overturn, *Deep Sea Res., Part II*, *48*, 1649–1667.

Huskin, I., L. Viesca, and R. Amadón (2004), Particle flux in the subtropical Atlantic near the Azores: Influence of mesozooplankton, *J. Plankton Res.*, *26*, 403–415.

Le Cann, B., M. Assenbaum, J.-C. Gascard, and G. Reverdin (2005), Observed mean and mesoscale upper ocean circulation in the midlatitude northeast Atlantic, *J. Geophys. Res.*, *110*, C07S05, doi:10.1029/2004JC002768.

Levitus, S. (1982), Climatological atlas of the world ocean, *NOAA Prof. Pap.*, *13*, 173 pp.

Lévy, M., Y. Lehahn, J.-M. André, L. Mémery, H. Loisel, and E. Heifetz (2005), Production regimes in the northeast Atlantic: A study based on Sea-viewing Wide Field-of-view Sensor (SeaWiFS) chlorophyll and ocean general circulation model mixed layer depth, *J. Geophys. Res.*, *110*, C07S10, doi:10.1029/2004JC002771.

Maixandeau, A., D. Lèfevre, C. Fernandez I., R. Sempéré, R. Sohrin, J. Ras, F. Van Wambeke, G. Caniaux, and B. Quéguiner (2005), Mesoscale and seasonal variability of community production and respiration in the surface waters of the N.E. Atlantic Ocean, *Deep Sea Res., Part I*, *52*, 1663–1676.

McCartney, M. S., and L. D. Talley (1982), The Subpolar Mode Water of the North Atlantic Ocean, *J. Phys. Oceanogr.*, *12*, 1169–1188.

Mémery, L., G. Reverdin, J. Paillet, and A. Oschlies (2005), Introduction to the POMME special section: Thermocline ventilation and biogeochem-

ical tracer distribution in the northeast Atlantic Ocean and impact of mesoscale dynamics, *J. Geophys. Res.*, *110*, C07S01, doi:10.1029/2005JC002976.

Ogawa, H., T. Usui, and I. Koike (2003), Distribution of dissolved organic carbon in the east China Sea, *Deep Sea Res., Part II*, *50*, 353–366.

Paillet, J., and M. Arhan (1996), Oceanic ventilation in the eastern North Atlantic, *J. Phys. Oceanogr.*, *26*, 2036–2052.

Reverdin, G., M. Assenbaum, and L. Prieur (2005), Eastern North Atlantic Mode Waters during POMME (September 2000–2001), *J. Geophys. Res.*, *110*, C07S04, doi:10.1029/2004JC002613.

Sarmiento, J. L., R. Murname, and C. L. Quéré (1995), Air-sea CO_2 transfer and the carbon budget of the North Atlantic, *Philos. Trans. R. Soc. London, Ser. B*, *348*, 211–219.

Sempéré, R., E. Dafner, F. van Wambeke, D. Lefèvre, C. Magen, S. Allègre, F. Bruyant, M. Bianchi, and L. Prieur (2003), Distribution and cycling of total organic cabon across the Almeria-Oran Front in the Mediterranean Sea: Implications for carbon cycling in the western basin, *J. Geophys. Res.*, *108*(C11), 3361, doi:10.1029/2002JC001475.

Siegenthaler, U., and J. L. Sarmiento (1993), Atmospheric carbon dioxide and the ocean, *Nature*, *365*, 119–125.

Tanoue, E. (1993), Distributional characteristics of DOC in the central equatorial Pacific, *J. Oceanogr.*, *49*, 625–639.

Teira, E., M. J. Pazó, P. Serret, and E. Fernández (2001), Dissolved organic carbon production by microbial population in the Atlantic Ocean, *Limnol. Oceanogr.*, *46*, 1370–1377.

Tian, R. C., D. Deibel, R. B. Rivkin, and A. F. Vézina (2004), Biogenic carbon and nitrogen export in a deep-convection region: Simulations in the Labrador Sea, *Deep Sea Res., Part I*, *51*, 413–437.

Tsuchiya, M., L. D. Talley, and M. S. McCartney (1992), An eastern Atlantic section from Iceland southward across the equator, *Deep Sea Res., Part A*, *39*, 1885–1917.

van Aken, H. M. (2000a), The hydrography of the mid-latitude northeast Atlantic Ocean I: The deep water masses, *Deep Sea Res., Part I*, *47*, 757–788.

van Aken, H. M. (2000b), The hydrography of the mid-latitude northeast Atlantic Ocean II: The intermediate water masses, *Deep Sea Res., Part I*, *47*, 789–824.

Vlasenko, V. I. (1994), Multimodal solution of internal waves, *Atmos. Oceanic Phys.*, *30*, 161–169.

Wiebinga, C. J., and H. J. W. de Baar (1998), Determination of the distribution of dissolved organic carbon in the Indian sector of the Southern Ocean, *Mar. Chem.*, *61*, 185–201.

R. Sempéré, Laboratoire de Microbiologie Géochimie et Ecologie Marines, CNRS/INSU, UMR 6117, Centre d'Océanologie de Marseille, Université de la Mediterranée, Campus de Luminy, Case 901, F-13288 Marseille Cedex 9, France. (sempere@com.univ-mrs.fr)

R. Sohrin, Institute of Geosciences, Shizuoka University, 836 Oya, Shizuoka 422-8529, Japan. (srsohri@ipc.shizuoka.ac.jp)